

A Search for the Higgs Boson Produced in Association with $Z \rightarrow \ell^+\ell^-$ Using the Matrix Element Method at CDF II

T. Aaltonen,²⁴ J. Adelman,¹⁴ T. Akimoto,⁵⁶ B. Álvarez González^{t,12} S. Amerio^{z,44} D. Amidei,³⁵ A. Anastassov,³⁹ A. Annovi,²⁰ J. Antos,¹⁵ G. Apollinari,¹⁸ A. Apresyan,⁴⁹ T. Arisawa,⁵⁸ A. Artikov,¹⁶ W. Ashmanskas,¹⁸ A. Attal,⁴ A. Aurisano,⁵⁴ F. Azfar,⁴³ W. Badgett,¹⁸ A. Barbaro-Galtieri,²⁹ V.E. Barnes,⁴⁹ B.A. Barnett,²⁶ P. Barria^{bb,47} V. Bartsch,³¹ G. Bauer,³³ P.-H. Beauchemin,³⁴ F. Bedeschi,⁴⁷ D. Beecher,³¹ S. Behari,²⁶ G. Bellettini^{aa,47} J. Bellinger,⁶⁰ D. Benjamin,¹⁷ A. Beretvas,¹⁸ J. Beringer,²⁹ A. Bhatti,⁵¹ M. Binkley,¹⁸ D. Bisello^{z,44} I. Bizjak^{ff,31} R.E. Blair,² C. Blocker,⁷ B. Blumenfeld,²⁶ A. Bocci,¹⁷ A. Bodek,⁵⁰ V. Boisvert,⁵⁰ G. Bolla,⁴⁹ D. Bortoletto,⁴⁹ J. Boudreau,⁴⁸ A. Boveia,¹¹ B. Brau^{a,11} A. Bridgeman,²⁵ L. Brigliadori^{y,6} C. Bromberg,³⁶ E. Brubaker,¹⁴ J. Budagov,¹⁶ H.S. Budd,⁵⁰ S. Budd,²⁵ S. Burke,¹⁸ K. Burkett,¹⁸ G. Busetto^{z,44} P. Bussey,²² A. Buzatu,³⁴ K. L. Byrum,² S. Cabrera^{v,17} C. Calancha,³² M. Campanelli,³⁶ M. Campbell,³⁵ F. Canelli^{14,18} A. Canepa,⁴⁶ B. Carls,²⁵ D. Carlsmith,⁶⁰ R. Carosi,⁴⁷ S. Carrillo^{n,19} S. Carron,³⁴ B. Casal,¹² M. Casarsa,¹⁸ A. Castro^{y,6} P. Catastini^{bb,47} D. Cauz^{ee,55} V. Cavaliere^{bb,47} M. Cavalli-Sforza,⁴ A. Cerri,²⁹ L. Cerrito^{p,31} S.H. Chang,²⁸ Y.C. Chen,¹ M. Chertok,⁸ G. Chiarelli,⁴⁷ G. Chlachidze,¹⁸ F. Chlebana,¹⁸ K. Cho,²⁸ D. Chokheli,¹⁶ J.P. Chou,²³ G. Choudalakis,³³ S.H. Chuang,⁵³ K. Chung^{o,18} W.H. Chung,⁶⁰ Y.S. Chung,⁵⁰ T. Chwalek,²⁷ C.I. Ciobanu,⁴⁵ M.A. Ciocci^{bb,47} A. Clark,²¹ D. Clark,⁷ G. Compostella,⁴⁴ M.E. Convery,¹⁸ J. Conway,⁸ M. Cordelli,²⁰ G. Cortiana^{z,44} C.A. Cox,⁸ D.J. Cox,⁸ F. Crescioli^{aa,47} C. Cuenca Almenar^{v,8} J. Cuevas^{t,12} R. Culbertson,¹⁸ J.C. Cully,³⁵ D. Dagenhart,¹⁸ M. Datta,¹⁸ T. Davies,²² P. de Barbaro,⁵⁰ S. De Cecco,⁵² A. Deisher,²⁹ G. De Lorenzo,⁴ M. Dell’Orso^{aa,47} C. Deluca,⁴ L. Demortier,⁵¹ J. Deng,¹⁷ M. Deninno,⁶ P.F. Derwent,¹⁸ A. Di Canto^{aa,47} G.P. di Giovanni,⁴⁵ C. Dionisi^{dd,52} B. Di Ruzza^{ee,55} J.R. Dittmann,⁵ M. D’Onofrio,⁴ S. Donati^{aa,47} P. Dong,⁹ J. Donini,⁴⁴ T. Dorigo,⁴⁴ S. Dube,⁵³ J. Efron,⁴⁰ A. Elagin,⁵⁴ R. Erbacher,⁸ D. Errede,²⁵ S. Errede,²⁵ R. Eusebi,¹⁸ H.C. Fang,²⁹ S. Farrington,⁴³ W.T. Fedorko,¹⁴ R.G. Feild,⁶¹ M. Feindt,²⁷ J.P. Fernandez,³² C. Ferrazza^{cc,47} R. Field,¹⁹ G. Flanagan,⁴⁹ R. Forrest,⁸ M.J. Frank,⁵ M. Franklin,²³ J.C. Freeman,¹⁸ I. Furic,¹⁹ M. Gallinaro,⁵² J. Galyardt,¹³ F. Garbersen,¹¹ J.E. Garcia,²¹ A.F. Garfinkel,⁴⁹ P. Garosi^{bb,47} K. Genser,¹⁸ H. Gerberich,²⁵ D. Gerdes,³⁵ A. Gessler,²⁷ S. Giagu^{dd,52} V. Giakoumopoulou,³ P. Giannetti,⁴⁷ K. Gibson,⁴⁸ J.L. Gimmell,⁵⁰ C.M. Ginsburg,¹⁸ N. Giokaris,³ M. Giordani^{ee,55} P. Giromini,²⁰ M. Giunta,⁴⁷ G. Giurgiu,²⁶ V. Glagolev,¹⁶ D. Glenzinski,¹⁸ M. Gold,³⁸ N. Goldschmidt,¹⁹ A. Golossanov,¹⁸ G. Gomez,¹² G. Gomez-Ceballos,³³ M. Goncharov,³³ O. González,³² I. Gorelov,³⁸ A.T. Goshaw,¹⁷ K. Goulianos,⁵¹ A. Gresele^{z,44} S. Grinstein,²³ C. Grosso-Pilcher,¹⁴ R.C. Group,¹⁸ U. Grundler,²⁵ J. Guimaraes da Costa,²³ Z. Gunay-Unalan,³⁶ C. Haber,²⁹ K. Hahn,³³ S.R. Hahn,¹⁸ E. Halkiadakis,⁵³ B.-Y. Han,⁵⁰ J.Y. Han,⁵⁰ F. Happacher,²⁰ K. Hara,⁵⁶ D. Hare,⁵³ M. Hare,⁵⁷ S. Harper,⁴³ R.F. Harr,⁵⁹ R.M. Harris,¹⁸ M. Hartz,⁴⁸ K. Hatakeyama,⁵¹ C. Hays,⁴³ M. Heck,²⁷ A. Heijboer,⁴⁶ J. Heinrich,⁴⁶ C. Henderson,³³ M. Herndon,⁶⁰ J. Heuser,²⁷ S. Hewamanage,⁵ D. Hidas,¹⁷ C.S. Hill^{e,11} D. Hirschbuehl,²⁷ A. Hocker,¹⁸ S. Hou,¹ M. Houlden,³⁰ S.-C. Hsu,²⁹ B.T. Huffman,⁴³ R.E. Hughes,⁴⁰ U. Husemann,⁶¹ M. Hussein,³⁶ J. Huston,³⁶ J. Incandela,¹¹ G. Introzzi,⁴⁷ M. Iori^{dd,52} A. Ivanov,⁸ E. James,¹⁸ D. Jang,¹³ B. Jayatilaka,¹⁷ E.J. Jeon,²⁸ M.K. Jha,⁶ S. Jindariani,¹⁸ W. Johnson,⁸ M. Jones,⁴⁹ K.K. Joo,²⁸ S.Y. Jun,¹³ J.E. Jung,²⁸ T.R. Junk,¹⁸ T. Kamon,⁵⁴ D. Kar,¹⁹ P.E. Karchin,⁵⁹ Y. Kato^{m,42} R. Kephart,¹⁸ W. Ketchum,¹⁴ J. Keung,⁴⁶ V. Khotilovich,⁵⁴ B. Kilminster,¹⁸ D.H. Kim,²⁸ H.S. Kim,²⁸ H.W. Kim,²⁸ J.E. Kim,²⁸ M.J. Kim,²⁰ S.B. Kim,²⁸ S.H. Kim,⁵⁶ Y.K. Kim,¹⁴ N. Kimura,⁵⁶ L. Kirsch,⁷ S. Klimenko,¹⁹ B. Knuteson,³³ B.R. Ko,¹⁷ K. Kondo,⁵⁸ D.J. Kong,²⁸ J. Konigsberg,¹⁹ A. Korytov,¹⁹ A.V. Kotwal,¹⁷ M. Kreps,²⁷ J. Kroll,⁴⁶ D. Krop,¹⁴ N. Krumnack,⁵ M. Kruse,¹⁷ V. Krutelyov,¹¹ T. Kubo,⁵⁶ T. Kuhr,²⁷ N.P. Kulkarni,⁵⁹ M. Kurata,⁵⁶ S. Kwang,¹⁴ A.T. Laasanen,⁴⁹ S. Lami,⁴⁷ S. Lammel,¹⁸ M. Lancaster,³¹ R.L. Lander,⁸ K. Lannon^{s,40} A. Lath,⁵³ G. Latino^{bb,47} I. Lazzizzera^{z,44} T. LeCompte,² E. Lee,⁵⁴ H.S. Lee,¹⁴ S.W. Lee^{u,54} S. Leone,⁴⁷ J.D. Lewis,¹⁸ C.-S. Lin,²⁹ J. Linacre,⁴³ M. Lindgren,¹⁸ E. Lipeles,⁴⁶ A. Lister,⁸ D.O. Litvintsev,¹⁸ C. Liu,⁴⁸ T. Liu,¹⁸ N.S. Lockyer,⁴⁶ A. Loginov,⁶¹ M. Loretiz^{z,44} L. Lovas,¹⁵ D. Lucchesi^{z,44} C. Luci^{dd,52} J. Lueck,²⁷ P. Lujan,²⁹ P. Lukens,¹⁸ G. Lungu,⁵¹ L. Lyons,⁴³ J. Lys,²⁹ R. Lysak,¹⁵ D. MacQueen,³⁴ R. Madrak,¹⁸ K. Maeshima,¹⁸ K. Makhoul,³³ T. Maki,²⁴ P. Maksimovic,²⁶ S. Malde,⁴³ S. Malik,³¹ G. Manca^{e,30} A. Manousakis-Katsikakis,³ F. Margaroli,⁴⁹ C. Marino,²⁷ C.P. Marino,²⁵ A. Martin,⁶¹ V. Martin^{k,22} M. Martínez,⁴ R. Martínez-Ballarín,³² T. Maruyama,⁵⁶ P. Mastrandrea,⁵² T. Masubuchi,⁵⁶ M. Mathis,²⁶ M.E. Mattson,⁵⁹ P. Mazzanti,⁶ K.S. McFarland,⁵⁰ P. McIntyre,⁵⁴ R. McNulty^{j,30} A. Mehta,³⁰ P. Mehtala,²⁴ A. Menzione,⁴⁷ P. Merkel,⁴⁹ C. Mesropian,⁵¹ T. Miao,¹⁸ N. Miladinovic,⁷ R. Miller,³⁶ C. Mills,²³ M. Milnik,²⁷ A. Mitra,¹ G. Mitselmakher,¹⁹ H. Miyake,⁵⁶ N. Moggi,⁶ C.S. Moon,²⁸ R. Moore,¹⁸ M.J. Morello,⁴⁷ J. Morlock,²⁷ P. Movilla Fernandez,¹⁸ J. Mülmenstädt,²⁹ A. Mukherjee,¹⁸ Th. Muller,²⁷ R. Mumford,²⁶ P. Murat,¹⁸ M. Mussini^{y,6} J. Nachtman^{o,18} Y. Nagai,⁵⁶ A. Nagano,⁵⁶ J. Naganoma,⁵⁶ K. Nakamura,⁵⁶ I. Nakano,⁴¹ A. Napier,⁵⁷ V. Necula,¹⁷ J. Nett,⁶⁰ C. Neu^{w,46} M.S. Neubauer,²⁵ S. Neubauer,²⁷ J. Nielsen^{g,29} L. Nodulman,² M. Norman,¹⁰ O. Norniella,²⁵ E. Nurse,³¹ L. Oakes,⁴³ S.H. Oh,¹⁷ Y.D. Oh,²⁸ I. Oksuzian,¹⁹ T. Okusawa,⁴² R. Orava,²⁴ K. Osterberg,²⁴ S. Pagan Griso^{z,44}

E. Palencia,¹⁸ V. Papadimitriou,¹⁸ A. Papaikonomou,²⁷ A.A. Paramonov,¹⁴ B. Parks,⁴⁰ S. Pashapour,³⁴ J. Patrick,¹⁸ G. Pauletta^{ee,55} M. Paulini,¹³ C. Paus,³³ T. Peiffer,²⁷ D.E. Pellett,⁸ A. Penzo,⁵⁵ T.J. Phillips,¹⁷ G. Piacentino,⁴⁷ E. Pianori,⁴⁶ L. Pinera,¹⁹ K. Pitts,²⁵ C. Plager,⁹ L. Pondrom,⁶⁰ O. Poukhov*,¹⁶ N. Pounder,⁴³ F. Prakoshyn,¹⁶ A. Pronko,¹⁸ J. Proudfoot,² F. Ptohos^{i,18} E. Pueschel,¹³ G. Punzi^{aa,47} J. Pursley,⁶⁰ J. Rademacker^{c,43} A. Rahaman,⁴⁸ V. Ramakrishnan,⁶⁰ N. Ranjan,⁴⁹ I. Redondo,³² P. Renton,⁴³ M. Renz,²⁷ M. Rescigno,⁵² S. Richter,²⁷ F. Rimondi^{y,6} L. Ristori,⁴⁷ A. Robson,²² T. Rodrigo,¹² T. Rodriguez,⁴⁶ E. Rogers,²⁵ S. Rolli,⁵⁷ R. Roser,¹⁸ M. Rossi,⁵⁵ R. Rossin,¹¹ P. Roy,³⁴ A. Ruiz,¹² J. Russ,¹³ V. Rusu,¹⁸ B. Rutherford,¹⁸ H. Saarikko,²⁴ A. Safonov,⁵⁴ W.K. Sakumoto,⁵⁰ O. Saltó,⁴ L. Santi^{ee,55} S. Sarkar^{dd,52} L. Sartori,⁴⁷ K. Sato,¹⁸ A. Savoy-Navarro,⁴⁵ P. Schlabach,¹⁸ A. Schmidt,²⁷ E.E. Schmidt,¹⁸ M.A. Schmidt,¹⁴ M.P. Schmidt*,⁶¹ M. Schmitt,³⁹ T. Schwarz,⁸ L. Scodellaro,¹² A. Scribano^{bb,47} F. Scuri,⁴⁷ A. Sedov,⁴⁹ S. Seidel,³⁸ Y. Seiya,⁴² A. Semenov,¹⁶ L. Sexton-Kennedy,¹⁸ F. Sforza^{aa,47} A. Sfyrla,²⁵ S.Z. Shalhout,⁵⁹ T. Shears,³⁰ R. Shekhar,¹⁷ P.F. Shepard,⁴⁸ M. Shimojima^{r,56} S. Shiraishi,¹⁴ M. Shochet,¹⁴ Y. Shon,⁶⁰ I. Shreyber,³⁷ P. Sinervo,³⁴ A. Sisakyan,¹⁶ A.J. Slaughter,¹⁸ J. Slaunwhite,⁴⁰ K. Sliwa,⁵⁷ J.R. Smith,⁸ F.D. Snider,¹⁸ R. Snihur,³⁴ A. Soha,⁸ S. Somalwar,⁵³ V. Sorin,³⁶ T. Spreitzer,³⁴ P. Squillacioti^{bb,47} M. Stanitzki,⁶¹ R. St. Denis,²² B. Stelzer,³⁴ O. Stelzer-Chilton,³⁴ D. Stentz,³⁹ J. Strologas,³⁸ G.L. Strycker,³⁵ J.S. Suh,²⁸ A. Sukhanov,¹⁹ I. Suslov,¹⁶ T. Suzuki,⁵⁶ A. Taffard^{f,25} R. Takashima,⁴¹ Y. Takeuchi,⁵⁶ R. Tanaka,⁴¹ M. Tecchio,³⁵ P.K. Teng,¹ K. Terashi,⁵¹ J. Thom^{h,18} A.S. Thompson,²² G.A. Thompson,²⁵ E. Thomson,⁴⁶ P. Tipton,⁶¹ P. Ttito-Guzmán,³² S. Tkaczyk,¹⁸ D. Toback,⁵⁴ S. Tokar,¹⁵ K. Tollefson,³⁶ T. Tomura,⁵⁶ D. Tonelli,¹⁸ S. Torre,²⁰ D. Torretta,¹⁸ P. Totaro^{ee,55} S. Tournear,⁴⁵ M. Trovato^{cc,47} S.-Y. Tsai,¹ Y. Tu,⁴⁶ N. Turini^{bb,47} F. Ukegawa,⁵⁶ S. Vallecorsa,²¹ N. van Remortel^{b,24} A. Varganov,³⁵ E. Vataga^{cc,47} F. Vázquez^{n,19} G. Velev,¹⁸ C. Vellidis,³ M. Vidal,³² R. Vidal,¹⁸ I. Vila,¹² R. Vilar,¹² T. Vine,³¹ M. Vogel,³⁸ I. Volobouev^{u,29} G. Volpi^{aa,47} P. Wagner,⁴⁶ R.G. Wagner,² R.L. Wagner,¹⁸ W. Wagner^{x,27} J. Wagner-Kuhr,²⁷ T. Wakisaka,⁴² R. Wallny,⁹ S.M. Wang,¹ A. Warburton,³⁴ D. Waters,³¹ M. Weinberger,⁵⁴ J. Weinelt,²⁷ W.C. Wester III,¹⁸ B. Whitehouse,⁵⁷ D. Whiteson^{f,46} A.B. Wicklund,² E. Wicklund,¹⁸ S. Wilbur,¹⁴ G. Williams,³⁴ H.H. Williams,⁴⁶ P. Wilson,¹⁸ B.L. Winer,⁴⁰ P. Wittich^{h,18} S. Wolbers,¹⁸ C. Wolfe,¹⁴ T. Wright,³⁵ X. Wu,²¹ F. Würthwein,¹⁰ S. Xie,³³ A. Yagil,¹⁰ K. Yamamoto,⁴² J. Yamaoka,¹⁷ U.K. Yang^{q,14} Y.C. Yang,²⁸ W.M. Yao,²⁹ G.P. Yeh,¹⁸ K. Yi^{o,18} J. Yoh,¹⁸ K. Yorita,⁵⁸ T. Yoshida^{l,42} G.B. Yu,⁵⁰ I. Yu,²⁸ S.S. Yu,¹⁸ J.C. Yun,¹⁸ L. Zanello^{dd,52} A. Zanetti,⁵⁵ X. Zhang,²⁵ Y. Zheng^{d,9} and S. Zucchelli^{y,6}

(CDF Collaboration[†])

¹*Institute of Physics, Academia Sinica, Taipei, Taiwan 11529, Republic of China*

²*Argonne National Laboratory, Argonne, Illinois 60439*

³*University of Athens, 157 71 Athens, Greece*

⁴*Institut de Física d'Altes Energies, Universitat Autònoma de Barcelona, E-08193, Bellaterra (Barcelona), Spain*

⁵*Baylor University, Waco, Texas 76798*

⁶*Istituto Nazionale di Fisica Nucleare Bologna, ^yUniversity of Bologna, I-40127 Bologna, Italy*

⁷*Brandeis University, Waltham, Massachusetts 02254*

⁸*University of California, Davis, Davis, California 95616*

⁹*University of California, Los Angeles, Los Angeles, California 90024*

¹⁰*University of California, San Diego, La Jolla, California 92093*

¹¹*University of California, Santa Barbara, Santa Barbara, California 93106*

¹²*Instituto de Física de Cantabria, CSIC-University of Cantabria, 39005 Santander, Spain*

¹³*Carnegie Mellon University, Pittsburgh, PA 15213*

¹⁴*Enrico Fermi Institute, University of Chicago, Chicago, Illinois 60637*

¹⁵*Comenius University, 842 48 Bratislava, Slovakia; Institute of Experimental Physics, 040 01 Kosice, Slovakia*

¹⁶*Joint Institute for Nuclear Research, RU-141980 Dubna, Russia*

¹⁷*Duke University, Durham, North Carolina 27708*

¹⁸*Fermi National Accelerator Laboratory, Batavia, Illinois 60510*

¹⁹*University of Florida, Gainesville, Florida 32611*

²⁰*Laboratori Nazionali di Frascati, Istituto Nazionale di Fisica Nucleare, I-00044 Frascati, Italy*

²¹*University of Geneva, CH-1211 Geneva 4, Switzerland*

²²*Glasgow University, Glasgow G12 8QQ, United Kingdom*

²³*Harvard University, Cambridge, Massachusetts 02138*

²⁴*Division of High Energy Physics, Department of Physics, University of Helsinki and Helsinki Institute of Physics, FIN-00014, Helsinki, Finland*

²⁵*University of Illinois, Urbana, Illinois 61801*

²⁶*The Johns Hopkins University, Baltimore, Maryland 21218*

²⁷*Institut für Experimentelle Kernphysik, Universität Karlsruhe, 76128 Karlsruhe, Germany*

²⁸*Center for High Energy Physics: Kyungpook National University, Daegu 702-701, Korea; Seoul National University, Seoul 151-742, Korea; Sungkyunkwan University, Suwon 440-746, Korea; Korea Institute of Science and Technology Information, Daejeon, 305-806, Korea; Chonnam National University, Gwangju, 500-757, Korea*

- ²⁹Ernest Orlando Lawrence Berkeley National Laboratory, Berkeley, California 94720
³⁰University of Liverpool, Liverpool L69 7ZE, United Kingdom
³¹University College London, London WC1E 6BT, United Kingdom
³²Centro de Investigaciones Energeticas Medioambientales y Tecnologicas, E-28040 Madrid, Spain
³³Massachusetts Institute of Technology, Cambridge, Massachusetts 02139
³⁴Institute of Particle Physics: McGill University, Montréal, Québec, Canada H3A 2T8; Simon Fraser University, Burnaby, British Columbia, Canada V5A 1S6; University of Toronto, Toronto, Ontario, Canada M5S 1A7; and TRIUMF, Vancouver, British Columbia, Canada V6T 2A3
³⁵University of Michigan, Ann Arbor, Michigan 48109
³⁶Michigan State University, East Lansing, Michigan 48824
³⁷Institution for Theoretical and Experimental Physics, ITEP, Moscow 117259, Russia
³⁸University of New Mexico, Albuquerque, New Mexico 87131
³⁹Northwestern University, Evanston, Illinois 60208
⁴⁰The Ohio State University, Columbus, Ohio 43210
⁴¹Okayama University, Okayama 700-8530, Japan
⁴²Osaka City University, Osaka 588, Japan
⁴³University of Oxford, Oxford OX1 3RH, United Kingdom
⁴⁴Istituto Nazionale di Fisica Nucleare, Sezione di Padova-Trento, ^zUniversity of Padova, I-35131 Padova, Italy
⁴⁵LPNHE, Université Pierre et Marie Curie/IN2P3-CNRS, UMR7585, Paris, F-75252 France
⁴⁶University of Pennsylvania, Philadelphia, Pennsylvania 19104
⁴⁷Istituto Nazionale di Fisica Nucleare Pisa, ^{aa}University of Pisa, ^{bb}University of Siena and ^{cc}Scuola Normale Superiore, I-56127 Pisa, Italy
⁴⁸University of Pittsburgh, Pittsburgh, Pennsylvania 15260
⁴⁹Purdue University, West Lafayette, Indiana 47907
⁵⁰University of Rochester, Rochester, New York 14627
⁵¹The Rockefeller University, New York, New York 10021
⁵²Istituto Nazionale di Fisica Nucleare, Sezione di Roma 1, ^{dd}Sapienza Università di Roma, I-00185 Roma, Italy
⁵³Rutgers University, Piscataway, New Jersey 08855
⁵⁴Texas A&M University, College Station, Texas 77843
⁵⁵Istituto Nazionale di Fisica Nucleare Trieste/Udine, I-34100 Trieste, ^{ee}University of Trieste/Udine, I-33100 Udine, Italy
⁵⁶University of Tsukuba, Tsukuba, Ibaraki 305, Japan
⁵⁷Tufts University, Medford, Massachusetts 02155
⁵⁸Waseda University, Tokyo 169, Japan
⁵⁹Wayne State University, Detroit, Michigan 48201
⁶⁰University of Wisconsin, Madison, Wisconsin 53706
⁶¹Yale University, New Haven, Connecticut 06520

We present a search for associated production of the standard model (SM) Higgs boson and a Z boson where the Z boson decays to two leptons and the Higgs decays to a pair of b quarks in $p\bar{p}$ collisions at the Fermilab Tevatron. We use event probabilities based on SM matrix elements to construct a likelihood function of the Higgs content of the data sample. In a CDF data sample corresponding to an integrated luminosity of 2.7 fb^{-1} we see no evidence of a Higgs boson with a mass between $100 \text{ GeV}/c^2$ and $150 \text{ GeV}/c^2$. We set 95% confidence level (C.L.) upper limits on the cross-section for ZH production as a function of the Higgs boson mass m_H ; the limit is 8.2 times the SM prediction at $m_H = 115 \text{ GeV}/c^2$.

PACS numbers: 14.80.Bn, 13.38.Dg, 13.85.Qk, 14.70.Hp

*Deceased

[†]With visitors from ^aUniversity of Massachusetts Amherst, Amherst, Massachusetts 01003, ^bUniversiteit Antwerpen, B-2610 Antwerp, Belgium, ^cUniversity of Bristol, Bristol BS8 1TL, United Kingdom, ^dChinese Academy of Sciences, Beijing 100864, China, ^eIstituto Nazionale di Fisica Nucleare, Sezione di Cagliari, 09042 Monserrato (Cagliari), Italy, ^fUniversity of California Irvine, Irvine, CA 92697, ^gUniversity of California Santa Cruz, Santa Cruz, CA 95064, ^hCornell University, Ithaca, NY 14853, ⁱUniversity of Cyprus, Nicosia CY-1678, Cyprus, ^jUniversity College Dublin, Dublin 4, Ireland, ^kUniversity of Edinburgh, Edinburgh EH9 3JZ, United Kingdom, ^lUniversity of Fukui, Fukui City, Fukui Prefecture, Japan 910-0017 ^mKinki University, Higashi-Osaka City, Japan 577-8502 ⁿUniversidad Iberoamericana, Mexico D.F., Mexico, ^oUniversity of

In the standard model (SM), the Higgs mechanism is responsible for the observed breaking of the $SU(2)_L \otimes U(1)$ symmetry [1, 2], yet the Higgs boson remains the only SM particle that has not been directly observed. Direct searches

Iowa, Iowa City, IA 52242, ^pQueen Mary, University of London, London, E1 4NS, England, ^qUniversity of Manchester, Manchester M13 9PL, England, ^rNagasaki Institute of Applied Science, Nagasaki, Japan, ^sUniversity of Notre Dame, Notre Dame, IN 46556, ^tUniversity de Oviedo, E-33007 Oviedo, Spain, ^uTexas Tech University, Lubbock, TX 79609, ^vIFIC(CSIC-Universitat de Valencia), 46071 Valencia, Spain, ^wUniversity of Virginia, Charlottesville, VA 22904, ^xBergische Universität Wuppertal, 42097 Wuppertal, Germany, ^{ff}On leave from J. Stefan Institute, Ljubljana, Slovenia,

have set a lower limit on the SM Higgs boson mass m_H of 114.4 GeV/ c^2 at 95% C.L. [3], while precision electroweak measurements indirectly constrain its mass to $m_H = 76^{+33}_{-24}$ GeV/ c^2 [4]. At hadron colliders the dominant production process for the SM Higgs boson is $gg \rightarrow H$ while its decays are dominated by $H \rightarrow b\bar{b}$ for $m_H < 140$ GeV/ c^2 . However, the process $gg \rightarrow H \rightarrow b\bar{b}$ is dwarfed by multi-jet background, necessitating the search for Higgs bosons produced in association with a W or Z boson that decays leptonically. This article reports a search for the process $p\bar{p} \rightarrow ZH \rightarrow \ell^-\ell^+b\bar{b}$ ($\ell = e, \mu$) in data with an integrated luminosity of 2.7 fb $^{-1}$ collected with the CDF II detector, nearly 3 times that of the previously reported analysis [5]. The study of Higgs boson production in association with a W/Z gauge boson for low Higgs boson masses is further motivated by the fact that the signal to background ratio is more favorable at the Tevatron compared to the Large Hadron Collider.

For the first time in a $ZH \rightarrow \ell^-\ell^+b\bar{b}$ search, we utilize a method based on leading-order matrix element calculations [6–8] convoluted with detector resolution functions [9] that form per-event likelihoods. This method, pioneered for use in top quark mass measurements [10, 11], has been recently used in Higgs boson searches in other decay channels [12] by forming a discriminating per-event variable. We extend the technique by expressing the event likelihoods as a function of the ZH signal fraction and maximizing the joint likelihood for the data sample with respect to the signal fraction.

The CDF II detector [13, 14] is an azimuthally and forward-backward symmetric apparatus designed to study $p\bar{p}$ collisions at the Fermilab Tevatron. It consists of a magnetic spectrometer surrounded by calorimeters and muon chambers. The charged particle tracking system, consisting of a silicon detector and drift chamber, is immersed in a 1.4 T magnetic field parallel to the p and \bar{p} beams. Calorimeters segmented in η and ϕ surround the tracking system and measure the energy of particles detected within them. The electromagnetic and hadronic calorimeters are lead-scintillator and iron-scintillator sampling devices, respectively. Drift chambers located outside the central hadron calorimeters detect muons. The data used in this analysis are collected with an online selection that requires events to have a lepton with $E_T > 18$ GeV (for an electron) or $p_T > 18$ GeV/ c (for a muon) [14].

The event selection used in this analysis closely follows that in Ref. [5]. Candidate events are required to have a pair of oppositely charged electrons or muons with invariant mass $76 < m_{\ell\ell} < 106$ GeV/ c^2 . Candidate events are also required to have one jet with $E_T > 25$ GeV and at least one additional jet with $E_T > 15$ GeV, both within $|\eta| < 2.0$. All jet energies are corrected for non-uniformities in calorimeter response, effects from multiple $p\bar{p}$ interactions and for the hadronic energy scale of the calorimeter [15]. Candidate events are required to have at least one jet with an associated displaced secondary vertex [16] (“ b -tags”, reconstructed using tracks with hits in the silicon detector), thus enriching the b -quark content of the sample.

TABLE I: Expected and observed numbers of events with 1 or 2 b -tagged jets in 2.7 fb $^{-1}$ of data. The ZH expectation is shown for $m_H = 115$ GeV/ c^2 assuming the production cross section at $\sqrt{s} = 1.96$ TeV for $q\bar{q} \rightarrow Z^* \rightarrow ZH$ to be 1.04 pb [20] and the branching ratio $\mathcal{B}(H \rightarrow b\bar{b})$ to be 73% [21].

Source	1 tag	≥ 2 tag
$Z \rightarrow \ell^+\ell^- + \text{light partons}$	129.6 ± 24.0	5.5 ± 0.9
$Z \rightarrow \ell^+\ell^- + b\bar{b}, c\bar{c}$	107.2 ± 14.0	19.5 ± 3.4
ZZ, WZ	11.6 ± 1.3	2.9 ± 0.4
$t\bar{t}$	13.9 ± 2.0	7.7 ± 1.1
Mis-ID lepton	15.9 ± 6.5	0.4 ± 0.2
ZH	1.3 ± 0.2	0.7 ± 0.1
Total expected	279.5 ± 28.6	36.3 ± 3.7
Data	258	32

The backgrounds for this analysis are dominated by events with real Z bosons with additional contributions from $t\bar{t}$ and events where an object, such as a jet, is mis-identified as a lepton. We model the backgrounds with events generated with leading-order event generators, normalized to next-to-leading order cross-sections and simulated with a GEANT-based description of the CDF II detector [9]. Z +light-flavor jet contributions are modeled with the ALPGEN [17] simulation code matched with PYTHIA in the MLM scheme [17] for the hadronization and fragmentation. Heavy flavor contributions from $Z + b\bar{b}$ and $Z + c\bar{c}$ are modeled separately with ALPGEN and combined with the light-flavor jet samples. The WZ , ZZ and $t\bar{t}$ processes are modeled using PYTHIA [18]. Events where a jet is mis-identified as a charged lepton are modeled using jet-enriched data samples [5, 19]. We model the kinematics of $ZH \rightarrow \ell^+\ell^-b\bar{b}$ events using PYTHIA for m_H ranging from 100 GeV/ c^2 to 150 GeV/ c^2 . The signal and background contributions expected in 2.7 fb $^{-1}$ and the number of observed events are given in Table I.

We denote the ZH signal probability by $P_{ZH}(\mathbf{x}_i|m_H)$ where m_H is a parameter and \mathbf{x}_i represents the collection of the measured 4-vector momenta of the two selected leptons, the two selected jets, and the two components of the missing transverse momentum, in a given event i . Similarly we denote the background probability as $P_b(\mathbf{x}_i)$. The per-event likelihood as a function of the signal fraction s for a given event i is

$$L(s, \mathbf{x}_i|m_H) = sP_{ZH}(\mathbf{x}_i|m_H) + (1-s)P_b(\mathbf{x}_i). \quad (1)$$

We evaluate P_{ZH} and P_b by convoluting the leading-order matrix elements for the process with detector resolution functions and integrating over unmeasured quantities. Thus, P_{ZH} is a probability density in \mathbf{x}_i and can be expressed as

$$P_{ZH}(\mathbf{x}_i|m_H) = \frac{1}{\sigma(m_H)} \int d\Phi |\mathcal{M}_{ZH}(q, p; m_H)|^2 \times \prod_j [W(p_j, \mathbf{x}_i)] f_{PDF}(q_1) f_{PDF}(q_2) \quad (2)$$

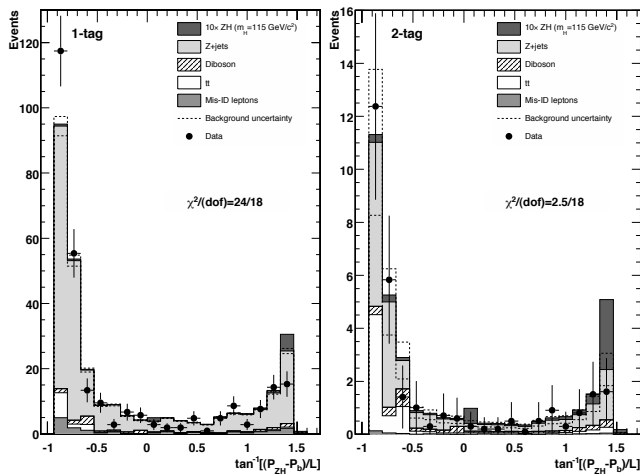


FIG. 1: The distribution of $\tan^{-1} \mathcal{D}$ where the discriminant $\mathcal{D} = (P_{ZH} - P_b)/L$ for expected backgrounds and data for events with one (left) and two (right) b -tags. The expected signal ($\times 10$) is overlaid.

where \mathcal{M}_{ZH} is the leading-order matrix element for the process $q\bar{q} \rightarrow ZH \rightarrow \ell^+\ell^-b\bar{b}$ evaluated for a pair of incoming partons q and outgoing particles p , $W(p_j, \mathbf{x}_i)$ are transfer functions [22] linking the outgoing particle momenta p_j to measured quantities \mathbf{x}_i and the f_{PDF} are parton density functions of the incoming partons. The factor $1/\sigma(m_H)$ ensures that the probability density satisfies the normalization condition, $\int d\mathbf{x}_i P_{ZH}(\mathbf{x}_i|m_H) = 1$.

The sample likelihood \mathcal{L} is obtained by taking the product over all events i in the sample

$$\mathcal{L}(s|m_H) = \prod_i L(s, \mathbf{x}_i|m_H). \quad (3)$$

We enhance our statistical sensitivity by exploiting the expected difference in the rate of signal and background events with two b -tagged jets. We replace $P_{ZH}(\mathbf{x}_i|m_H)$ by $P_{ZH}(\mathbf{x}_i, n|m_H) \equiv P_{ZH}(\mathbf{x}_i|m_H) \cdot P_{ZH}(n|m_H)$ and $P_b(\mathbf{x}_i)$ by $P_b(\mathbf{x}_i, n) \equiv P_b(\mathbf{x}_i) \cdot P_b(n)$, where $P_{ZH}(n|m_H)$ [$P_b(n)$] denotes the probability of tagging signal [background] events with n tags. Table II shows the expected tagging rates for simulated signal and background event samples.

The measured signal fraction S_{meas} is the value of s which maximizes $\mathcal{L}(s|m_H)$. Using Eq. (1), we can define a per-event discriminant $\mathcal{D}_i \equiv \partial \ln L / \partial s = (P_{ZH} - P_b)/L$ which increases (decreases) for more signal-like (background-like) events. The maximum-likelihood estimator for the measured signal fraction S_{meas} corresponds to $\sum_i \mathcal{D}_i|_{s=S_{meas}} = 0$. The distribution of $\tan^{-1} \mathcal{D}_i$ ($s = S_{meas}$) for simulated events and data is shown in Fig. 1.

The dominant backgrounds in our data sample are due to Z +jets, $t\bar{t}$ and ZZ processes, in the expected proportions denoted by λ_{Zjj} , $\lambda_{t\bar{t}}$ and λ_{ZZ} respectively. The background probability in Eq. (1) is given by

TABLE II: Expected single- and double-tag probabilities, $P(n=1)$ and $P(n \geq 2)$, for signal and background events passing our selection. $Z \rightarrow \ell^+\ell^-$ +jets includes jets from both light and heavy quarks.

Source	$P(n=1)$	$P(n \geq 2)$
$Z \rightarrow \ell^+\ell^-$ +jets	0.91	0.09
WZ, ZZ	0.80	0.20
$t\bar{t}$	0.74	0.26
ZH ($m_H = 100 \text{ GeV}/c^2$)	0.67	0.33
ZH ($m_H = 125 \text{ GeV}/c^2$)	0.65	0.35
ZH ($m_H = 150 \text{ GeV}/c^2$)	0.63	0.37

$$P_b(\mathbf{x}_i, n) = \lambda_{Zjj} P_{Zjj}(\mathbf{x}_i, n) + \lambda_{t\bar{t}} P_{t\bar{t}}(\mathbf{x}_i, n) + \lambda_{ZZ} P_{ZZ}(\mathbf{x}_i, n), \quad (4)$$

where $P_{Zjj}(\mathbf{x}_i, n)$, $P_{t\bar{t}}(\mathbf{x}_i, n)$ and $P_{ZZ}(\mathbf{x}_i, n)$ are the respective probability densities (normalized to unit integral) for the Z +jets, $t\bar{t}$, and ZZ background processes with n tags. Normalization of P_b is ensured by requiring $\lambda_{Zjj} + \lambda_{t\bar{t}} + \lambda_{ZZ} = 1$.

We construct confidence intervals [23] for the test statistic $R = \mathcal{L}(S_{meas}|S_{true})/\mathcal{L}(S_{meas}|S_{true}^{best})$ by performing simulated experiments with the expected proportions of background and varying the amounts of signal, such that S_{true} is the true (input) signal fraction in the simulated experiment. S_{true}^{best} is the input signal fraction that has the highest likelihood for a given measured signal fraction, S_{meas} . $\mathcal{L}(S_{meas}|S_{true})$ is given by Eq. (3) for the simulated experiment with the chosen value of S_{true} and m_H . Since we are measuring the fractional signal content in the data sample, the number of events in each simulated experiment is held fixed at the value of 290 events observed in the data.

The methodology from Ref. [23] is used to construct confidence intervals in S_{meas} for each chosen value of S_{true} and m_H . This method removes any bias resulting from imperfections in our modeling by relating S_{meas} to S_{true} . The confidence intervals in S_{meas} obtained for $m_H = 115 \text{ GeV}/c^2$ and $0 \leq S_{true} \leq 0.25$ are shown in Fig. 2. For a given value of S_{meas} obtained from the data (or from an independent simulated experiment to evaluate the *a priori* expectation), we extract the range of S_{true} for which the confidence intervals contain this value of S_{meas} . A feature of this method is that the resulting range of S_{true} can be quoted as an upper limit on S_{true} (if the lower bound is zero) or as a two-sided measurement of S_{true} . As Fig. 2 shows, we obtain an upper limit on S_{true} given the data, which we convert to the equivalent upper limit on the signal cross section. This procedure is repeated for the range of Higgs boson masses $100 \leq m_H \leq 150 \text{ GeV}/c^2$.

We evaluate systematic uncertainties by varying process rates and kinematic distributions in our simulated experiments. We apply a rate uncertainty of 40% for Z boson events and of 20% for diboson and $t\bar{t}$ events. The uncertainty on the rate of heavy flavor production in association with a gauge boson is based on comparisons of data with theoretical predictions [19]. The uncertainty on the diboson and $t\bar{t}$ contribution

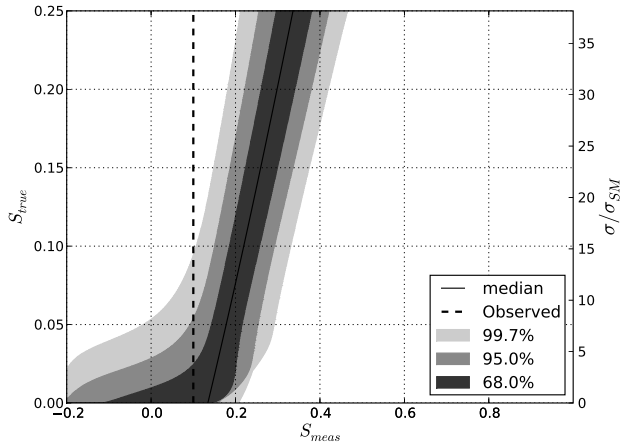


FIG. 2: Confidence intervals in the measured signal fraction S_{meas} (along the x -axis) with 68% C.L., 95% C.L. and 99.7% C.L., for a range of true signal fraction S_{true} values (along the y -axis on the left) chosen in the simulated experiments. The signal cross section ratio equivalent to S_{true} is shown on the y -axis on the right. The intervals shown here are computed for a Higgs boson mass of $m_H = 115 \text{ GeV}/c^2$, and include statistical and systematic uncertainties. The vertical dashed line indicates the value of S_{meas} obtained from the data.

includes the uncertainties in the cross sections, selection efficiencies and the top quark mass [5]. A rate uncertainty of 50% is applied for mis-identified lepton events due to the uncertainty on the lepton misidentification probability [5]. A rate uncertainty of 6% due to the luminosity uncertainty is applied to all events. The per-jet uncertainty on the b -tagging efficiency is 8% for events with b partons, 16% for events with c partons and 13% for events with no heavy flavor [5]. Our analysis is weakly sensitive to uncertainties in the expected total number of events passing our selection, since it relies only on the shapes of measured distributions. Uncertainties in the shapes of kinematic distributions are propagated by varying the amount of QCD radiation in simulated signal events and the jet energy scale in simulated signal and background events within their respective uncertainties [15].

We evaluate confidence intervals for a range of Higgs masses between $100 \text{ GeV}/c^2$ and $150 \text{ GeV}/c^2$. We evaluate *a priori* 95% C.L. upper limits on the cross section for the process $p\bar{p} \rightarrow ZH \rightarrow \ell^+\ell^-b\bar{b}$. We express these limits as a ratio with respect to the SM prediction. These expected limits along with those observed in the data are shown in Table III.

In conclusion, we have performed a search for the SM Higgs boson decaying to $b\bar{b}$ produced in association with a Z boson. This is the first analysis performed in this channel with a matrix element method. The data show no excess over expected non-Higgs backgrounds. We set 95% C.L. upper limits on the cross section of this process for a range of Higgs boson masses. The limit at $m_H = 115 \text{ GeV}/c^2$ is 8.2 times greater than the SM prediction. This result improves

TABLE III: Upper limits at 95% C.L. on the $ZH \rightarrow \ell^+\ell^-b\bar{b}$ cross section, shown as a ratio to the SM cross section. The column labelled “Expected” shows the median of the limits obtained from simulated experiments containing no signal, and the columns labelled “ $\pm 1\sigma$ ” show the range containing 68% of the expected limits.

m_H [GeV/ c^2]	-1σ [σ/σ_{SM}]	Expected [σ/σ_{SM}]	$+1\sigma$ [σ/σ_{SM}]	Observed [σ/σ_{SM}]
100	6.0	8.7	12.4	7.0
105	6.0	8.7	12.9	6.5
110	7.5	11.3	16.8	7.6
115	8.3	12.1	18.2	8.2
120	9.3	13.5	20.0	9.0
125	13.2	18.3	27.1	13.2
130	17.1	24.2	35.7	17.7
135	21.8	31.0	44.8	22.9
140	31.0	44.3	65.4	32.0
145	42.8	61.6	89.9	43.1
150	73.7	104	153	71.3

by a factor of 2 over the previously published result in this channel [5]. We are exploring further improvements in this technique by separating the leading-order and next-to-leading order contributions to the signal and backgrounds, as well as the use of matrix-element-based probabilities in conjunction with other multivariate discriminants.

We thank the Fermilab staff and the technical staffs of the participating institutions for their vital contributions. This work was supported by the U.S. Department of Energy and National Science Foundation; the Italian Istituto Nazionale di Fisica Nucleare; the Ministry of Education, Culture, Sports, Science and Technology of Japan; the Natural Sciences and Engineering Research Council of Canada; the National Science Council of the Republic of China; the Swiss National Science Foundation; the A.P. Sloan Foundation; the Bundesministerium für Bildung und Forschung, Germany; the World Class University Program, the National Research Foundation of Korea; the Science and Technology Facilities Council and the Royal Society, UK; the Institut National de Physique Nucleaire et Physique des Particules/CNRS; the Russian Foundation for Basic Research; the Ministerio de Ciencia e Innovación, and Programa Consolider-Ingenio 2010, Spain; the Slovak R&D Agency; and the Academy of Finland.

- [1] P. W. Higgs, Phys. Rev. Lett. **13**, 508 (1964).
- [2] G. S. Guralnik, C. R. Hagen, and T. W. B. Kibble, Phys. Rev. Lett. **13**, 585 (1964).
- [3] R. Barate *et al.* (LEP Working Group), Phys. Lett. B **565**, 61 (2003).
- [4] T. Aaltonen *et al.* (CDF Collaboration), Phys. Rev. D **77**, 112001 (2008).
- [5] T. Aaltonen *et al.* (CDF Collaboration), Phys. Rev. Lett. **101**, 251803 (2008).
- [6] J. M. Campbell and R. K. Ellis, Phys. Rev. D **60**, 113006

- (1999).
- [7] J. Alwall *et al.*, *J. High Energy Phys.* **0709**, 028 (2007).
- [8] G. Mahlon and S. Parke, *Phys. Lett. B* **411**, 173 (1997).
- [9] T. Affolder *et al.*, *Nucl. Instrum. Methods A* **447**, 1 (2000).
- [10] A. Abulencia *et al.* (CDF Collaboration), *Phys. Rev. Lett.* **96**, 152002 (2006).
- [11] V. Abazov *et al.* (DØ Collaboration), *Nature* **429**, 638 (2004).
- [12] T. Aaltonen *et al.* (CDF Collaboration), *Phys. Rev. Lett.* **102**, 021802 (2009).
- [13] D. Acosta *et al.* (CDF Collaboration), *Phys. Rev. D* **71**, 032001 (2005).
- [14] CDF uses a cylindrical coordinate system with the z axis along the proton beam axis. Pseudorapidity is $\eta \equiv -\ln(\tan\theta/2)$, where θ is the polar angle, and ϕ is the azimuthal angle relative to the proton beam direction, while $p_T = |p| \sin\theta$, $E_T = E \sin\theta$.
- [15] A. Bhatti *et al.*, *Nucl. Instrum. Methods A* **566**, 375 (2006).
- [16] D. Acosta *et al.* (CDF Collaboration), *Phys. Rev.* **71**, 052003 (2005).
- [17] M. L. Mangano *et al.*, *J. High Energy Phys.* **0307**, 001 (2003).
- [18] T. Sjostrand *et al.*, *Comput. Phys. Commun.* **135**, 238 (2001).
- [19] A. Abulencia *et al.* (CDF Collaboration), *Phys. Rev. D* **74**, 032008 (2006).
- [20] S. Catani, D. de Florian, M. Grazzini, and P. Nason, *J. High Energy Phys.* **2003**, 028 (2003).
- [21] A. Djouadi, J. Kalinowski, and M. Spira, *Comput. Phys. Commun.* **108**, 56 (1998), ISSN 0010-4655.
- [22] A. Abulencia *et al.* (CDF Collaboration), *Phys. Rev. D* **74**, 032009 (2006).
- [23] G. J. Feldman and R. D. Cousins, *Phys. Rev. D* **57**, 3873 (1998).